Smart microgels investigated by super-resolution fluorescence microscopy: Influence of the monomer structure on the particle morphology.

Oliver Wrede,[a,†] Stephan Bergmann,[b,†] Yvonne Hannappel,[a] Thomas Huser*[b] and Thomas Hellweg*[a]

In a recent publication [Bergmann et al. Phys. Chem. Chem. Phys., 2018,20, 5074-5083] we presented a method which enables to investigate the morphology of microgels by superresolution fluorescence microscopy. Here is, method is applied to three microgels species, based on *N*-isopropylmethacrylamide (NIPMAM), *N*-*n*-propylacrylamide (NNPAM) and *N*-*n*-propylmethacrylamide (NNPMAM)) with 5, 7.5 and 10 mol% cross-linker respectively. Super-resolution microscopy reveals differences of the network morphology of the synthesized particles showing the importance of the monomer structure.

Electronic supplementary information

S1 Experimental methods

S1.1 *d*STORM imaging

S1.1.1 Experimental setup

The experiments were performed with an argon krypton ion laser source (70C-Spectrum, Coherent Inc. Santa Clara, CA, USA) with selected 514 nm laser line through an acousto-optically tunable filter (AOTF) (OTFnC-VIS-TN, A-AOpto Electronic, Orsay, France). In addition, a laser cleaning filter (Z514 /10 X, Chroma) is used to suppress transmitted light through the AOTF. The laser light is focused on the back focal plane of a 60x TIRF objective (60x NA 1.49 ApoN, Olympus), mounted on a nosepiece stage (IX2-NPS; Olympus) to minimize axial drift between sample and objective, to obtain an almost homogeneous illumination (Gaussian intensity distribution). With a mirror in front of the upper rear port of the microscope body (IX 71, Olympus), the illumination scheme can be changed between Total Internal Reflection (TIR), strongly inclined and laminated optical plate (HILO) [1] and epifluorescence (EPI) depending on the position of the laser focus in the back focal plane. The first separation of the excitation light from the fluorescence and reflection of the excitation light is performed by a dichroic mirror (DCXR 540, Chroma). In order to adapt the cameras (IDS UI-3270CP Rev.2, IDS, Germany) physical pixel size of 3.45 μm to a desired image value according to the Point Spread Functions (PSF) standard deviation, which in practice is a pixel size between 100 nm/pixel and 160 nm/pixel, a telescope (f=300 mm and f=160 mm) in the 4f configuration was included in the detection path. A cylindrical lens (Thorlabs f = 1000 mm, Ø1", N-BK7 mounted planoconvex round cylinder lens, ARC 350-700) introduces a slight astigmatism, which is used to enable 3D *d*STORM [2]. The fluorescence signal is filtered by a combination of a long pass filter (532 nm LP Edge Basic, BLP01-532R-25, Semrock) and a bandpass filter (FF01-580/60-25-D Bandpass, Semrock).

S1.1.2 3D calibration

An custom written beanshell script for Micromanager is used to control a PIFOC (PIFOC P-721.10, PI). In 10 nm steps images of a fluorescent bead slide are acquired. Typically the PIFOC is moved over a range of 2μm. The function signal for the closed loop driven piezo driver (E-662.LR LVPZT Amplifier/ Position Controller, PI) is provided by a National Instruments PCIe card (NI PCIe-6259, National Instruments). The obtained z-stack is then evaluated by the calibration function in ThunderSTORM[3], where the improved version by Martens et al. [4] is used.

S1.1.3 Image acquisition

Due to the size of the microgels around 600 to 800 nm TIR is insufficient for imaging of the whole microgel. Therefore, HILO was used as the illumination scheme. This has the benefit of a high laser power density between 4 $kW cm^{-2}$ and 5 $kW cm^{-2}$ in the highly inclined and laminated optical sheet and the capability of suppressing the signal from free diffusing R6G molecules within the imaging buffer. For microgels with a transition temperate below the room temperature of 21 °C the sample temperature was cooled down with an ice-pack on the metal objective plate. The temperature was measured during the whole experiment with a thermometer (HH506RA, OMEGA, Germany), where the thermoelement is placed inside the imaging buffer. The camera is controlled via Micromanager with a

[a] *Physical and Biophysical Chemistry, Department of Chemistry, Bielefeld University, Universitätsstraße 25, 33615 Bielefeld, Germany*
[b] *Biomolecular Photonics, Department of Physics, Bielefeld University, Universitätsstraße 25, 33615 Bielefeld, Germany*
∗Corresponding authors: *thomas.huser@physik.uni-bielefeld.de, thomas.hellweg@uni-bielefeld.de*
† These authors contributed equally to this work.

modified device adapter by Marcel Müller *. In total for every data set 50000 images with a frequency of 50 Hz were recorded.

S1.1.4 *d*STORM imaging buffer

A sparse density of molecules in the fluorescent "on-state" is obtained by a so called *d*STORM imaging buffer containing an enzymatic oxygen scavenger system combined with a thiol, in this case 1M cysteamine hydrochloride (part number: M6500, Sigma Aldrich) (MEA) adjusted to pH 7.4 with 25% hydrochloric acid or 1M potassium hydroxide. The concentration in the final buffer were 60 U/mL catalase (Sigma Aldrich) and 5 U/mL glucose oxidase (Sigma Aldrich), 100 mM MEA. A small drop, typically 20 μl imaging *d*STROM buffer was added to the prepared sample slide.

S1.1.5 Image reconstruction with ThunderSTORM

For the reconstruction in ThunderSTORM a wavelet filter with the scale of two and the order of three was selected to find local maxima with the threshold of the 1st wavelet level of the input image. The localization of single emitters was then executed by elliptical Gaussian fits, with a fitting radius of 5 pixel and the method of weighted least squares. The obtained localization table is afterwards post processed only by a drift correction with the in build cross correlation method. Therefore, the a reconstruction with a final magnification of 5 times was chosen. The acquired 50000 images are divided into bins of 2500 frames and resulting drift correction was smoothed with a factor of 0.25. For finding the single microgels an image with adjusted contrast and brightness was used to make it easier for the imfindcircle function to localize the single microgels. For the later evaluation the obtained localization table was used.

S2 Results and Discussion

S2.1 Total numbers of evaluated microgels for *d*STORM localization density measurement

Table S1 Total number of microgels taken into account for the evaluation of the localization density in microgels synthesized with different polymers.

	5 mol% BIS	7.5 mol% BIS	10 mol% BIS
NNPMAM	5548	2857	760
NNPAM	10519	27168	40212
NIPMAM	6019	426	1719

S2.2 Average number of localizations of each microgel type

The average number of localizations per microgel for each microgel type can be calculated based on the available 2D localization density, which is calculated before the recalculation to a 3D localization density. The 2D localization density is calculated based on 10 nm thick ring segments.

Table S2 Average number of localizations per microgel. The calculation was done based on the 2D localization density. From the 3D localization density graphs the outer-most radius for the microgel was estimated. The used criteria is here the beginning plateau in the localization density.

NNPMAM: 5 mol% BIS 300 nm, 7.5 mol% BIS 300 nm, 10 mol% BIS 300 nm
NNPAM: 5 mol% BIS 350 nm, 7.5 mol% BIS 300 nm, 10 mol% BIS 380 nm
NIPMAM: 5 mol% BIS 400 nm, 7.5 mol% BIS 350 nm, 10 mol% BIS 350 nm

	5 mol% BIS	7.5 mol% BIS	10 mol% BIS
NNPMAM	17755 ± 29	6940 ± 27	25671 ± 86
NNPAM	11523 ± 19	8847 ± 5	17000 ± 7
NIPMAM	27500 ± 22	23916 ± 52	15890 ± 31

S2.3 Height estimation

S2.3.1 Height estimation from localization distributions

Additional to the lateral position of a fluorescent marker, the axial position can be encoded via astigmatism by inserting a cylindrical lens in the detection path. Therefore, it's possible to have an orthogonal view (xz- or yz-projections) on the microgel. Here we chose the xz-projection to do an estimation for the height of the microgel by taking a line plot through the middle of the microgel along the

*https://github.com/biophotonics-bielefeld/ids-device-adapter/releases/tag/v0.11

z-axis. This distribution can be fitted with a Gaussian distribution of the kind

$$f(x) = A \cdot \exp^{-0.5\left(\frac{(x-x_c)}{\sigma}\right)^2} + B, \tag{1}$$

with A the amplitude, x the position, x_c the center position, σ the standard deviation and B the offset. The error corresponds to the fitting error, but due to the higher localization uncertainty in axial direction the error has to be assumed around 50 nm or more.

S2.3.2 Ratio between microgel height and width

Instead of taking the Gaussian distribution over the localization distribution in the microgels, it's also possible to approximate the total height of the microgel by adding an ellipse to the xz-projection. Additionally it's possible to calculate the ration between the width and the height to estimate the microgels deformation (flattening). The added ellipses to the xz-projections shown in Fig.2, but modified by changing the brightness and contrast to facilitate the shape estimation.

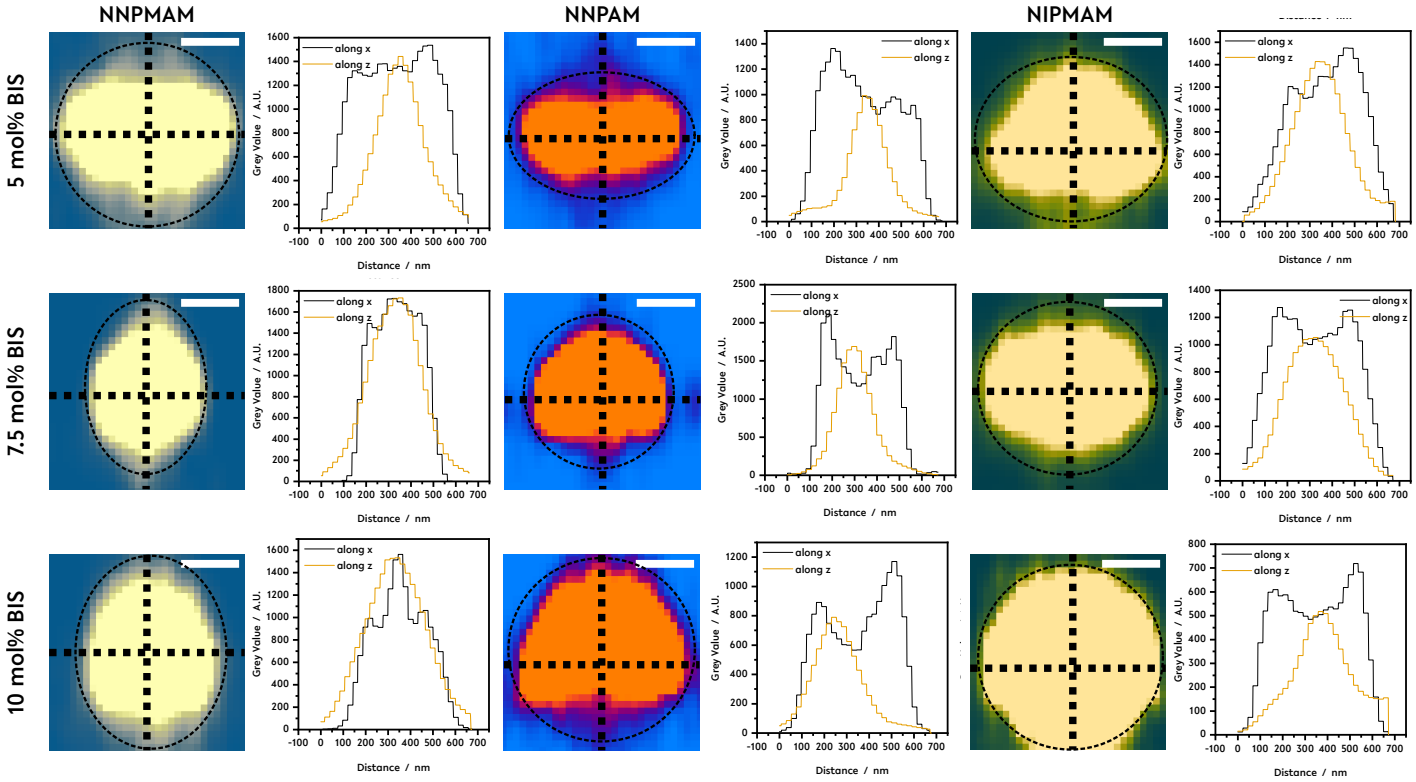

Fig. S1 The ratio between the height and the width of the microgels is measured based on the xz-projection of the microgels shown already in Fig.2. In this images the brightness and contrast are adjusted to facilitate the microgels shape. Along the x- and the z-axis a line plot shows the number of localizations as an arbitrary unit deviated from the grey scales. For an estimate of the width-height ratio an ellipse is added to the xz-projection. The length of the major and minor axis is used to calculate the ratio given in Tab.S3. Scale bar 200 nm

Table S3 This table shows the ratio between height and width of each microgel presented in Fig.2 and Fig.S1.

Ratio $\frac{width}{height}$	5 mol% BIS	7.5 mol% BIS	10 mol% BIS
NNPMAM	1.00	0.77	0.79
NNPAM	1.46	1	0.98
NIPMAM	1.17	1.03	1

References

1 M. Tokunaga, N. Imamoto and K. Sakata-Sogawa, *Nature methods*, 2008, **5**, 159–161.
2 B. Huang, W. Wang, M. Bates and X. Zhuang, *Science (New York, N.Y.)*, 2008, **319**, 810–813.
3 M. Ovesný, P. Křížek, J. Borkovec, Z. Svindrych and G. M. Hagen, *Bioinformatics (Oxford, England)*, 2014, **30**, 2389–2390.
4 K. J. A. Martens, A. N. Bader, S. Baas, B. Rieger and J. Hohlbein, *The Journal of Chemical Physics*, 2018, **148**, 123311.